Nonequilibrium Radiative Heating during Outer Planet Atmospheric Entry

H.F. Nelson*
University of Missouri-Rolla, Rolla, Missouri

Nomenclature

c	= speed of light
h	= Planck's constant
k	= Boltzmann's constant
n_e, n_H	= number density of electrons, hydrogen atoms
$n_H(2)$	= number density of first excited state
S_ν	= radiation source function
T_a, T_e	= temperature of atoms, electrons
$q_R(0,\nu)$	= radiative flux at heat shield
y	= shock-layer coordinate
δ_0	= shock-layer thickness
η	= nondimensional length y/δ_0
ν	= frequency
σ_{2f}	= excited state cross section
τ_ν^0	= optical thickness of shock layer at frequency ν

Introduction

THE design of the heat shield for a probe entering the atmosphere of Jupiter or Saturn is controlled by the radiation heat transfer. At present, the heat shield design is based on analytical models of the flowfield and heat-transfer phenomena, because experimental facilities capable of producing the extreme thermodynamic conditions of Jupiter and Saturn entry are not available. To improve the heat-transfer predictions, Leibowitz,[1] Leibowitz and Kuo,[2] and Tiwari and Szema[3,4] investigated the influence of finite-rate ionization on the radiative heating of probes entering the atmospheres of Jupiter and Saturn. However, they reached opposite conclusions. Tiwari and Szema[3,4] found that the radiation heating increased, whereas Leibowitz and Kuo[1,2] found that it decreased relative to the results obtained when the ionization rate was assumed to be in equilibrium at the local thermodynamic conditions.

This Note presents the underlying reasons for the opposite conclusions. The study is limited to stagnation shock layers for nonviscous, hydrogen-helium plasmas with cold, non-blowing conditions at the probe heat shield. The effects of ablation and the ablation-layer gases are not considered.

Equilibrium Modeling

The equilibrium model assumes that the atomic electronic states are populated with a Boltzmann distribution at the local temperature. The electron population is related to the atom and ion populations by the Saha equation. The plasma has a single temperature and all populations adjust instantly to any change in pressure or temperature. The radiation source function is the Planck function.

Nonequilibrium Modeling

The nonequilibrium model assumes that the shock layer consists of an electron gas and an atom gas (heavy particles, atoms, and ions). The electron gas and atom gas are allowed to have different temperatures (thermal nonequilibrium). The difference in their temperatures is controlled by collisional and radiative energy exchange processes, including ionization and excitation rates. The two gases relax toward equilibrium as they move away from the shock wave.

Leibowitz[1] developed a set of finite ionization and excitation rates assuming that the atomic gases in the shock layer have two bound electronic states: a ground state and an excited state. The single excited state represents all excited states. This assumption is justifiable for atomic hydrogen-helium shock layers, because the ground and first excited states of the atoms are separated by a large energy gap compared to the energy necessary to ionize an electron from the first excited state. For these gases the excited states and electrons have nearly the same energy. Thus, he also assumed the excited state and electron populations to be in equilibrium at the electron temperature. Consequently, the electron gas is not populated at its equilibrium value (ionizational nonequilibrium), and the excited states are not populated at their equilibrium value (excitational nonequilibrium).

Typical Solutions

Figure 1 shows a typical solution for the electron and atom temperature. Note that T_e and T_a are both greater than the equilibrium temperature just behind the shock ($\eta = 1$), whereas near the body ($\eta = 0$) the temperature is essentially the same for thermal equilibrium and nonequilibrium. The nonequilibrium shock layer is in thermal equilibrium for values of η less than 0.7.

Figure 2 shows that the electron density increases very slowly behind the shock for finite-rate ionization (nonequilibrium) as compared to the equilibrium solution. The excited state population behaves in a similar manner for finite-rate excitation. These differences are important when radiative emission is considered, because it is sensitive to n_e and $n_H(2)$. Also, for finite-rate ionization, the atomic hydrogen population is much higher just behind the shock than the equilibrium hydrogen population.

Figure 3 shows typical values of the shock-layer optical thickness as a function of the photon energy $h\nu$. In general, the shock layer is optically thin in the 1-9 eV spectral region. It is optically thick at the Lyman line at about 10 eV and for the Lyman continuum at energies greater than 13.6 eV. The shock layer is also optically thick for free-free continuum radiation at very low values of photon energy. The lower part of Fig. 3 shows the spectral position of the maximum in the Planck

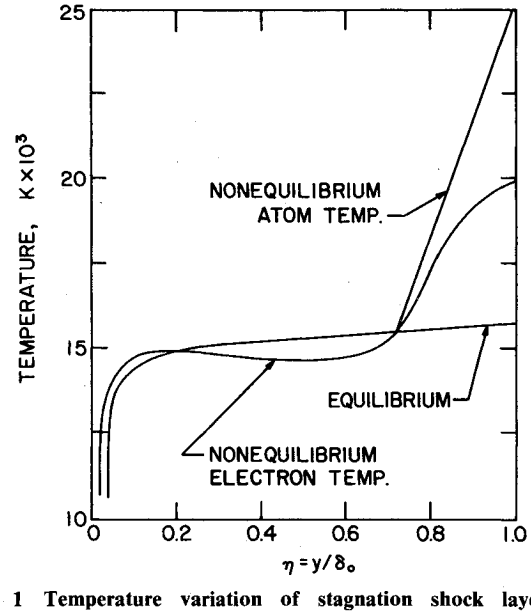

Fig. 1 Temperature variation of stagnation shock layer for equilibrium and finite-rate ionization for an 85% H_2 atmosphere (by volume) and a nose radius of 23 cm at an altitude of 116 km (from Ref. 4).

Received Oct. 8, 1982; revision received Jan. 24, 1983.

*Professor of Aerospace Engineering, Thermal Radiative Transfer Group, Department of Mechanical and Aerospace Engineering. Associate Fellow AIAA.

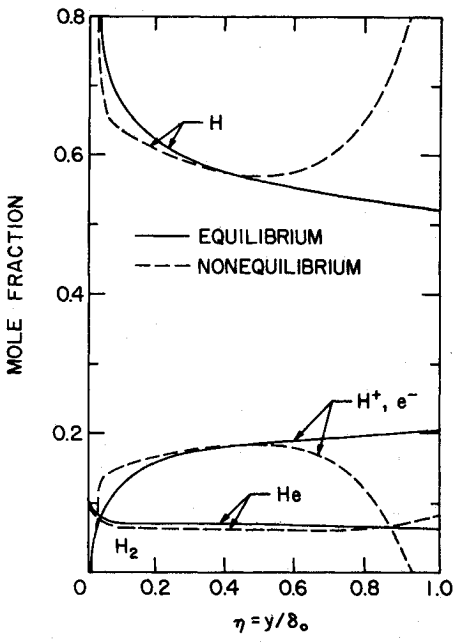

Fig. 2 Species mole fraction variation as a function of nondimensional position across the stagnation shock layer for an 85% H_2 atmosphere (by volume) and a nose radius of 23 cm at an altitude of 116 km (from Ref. 4).

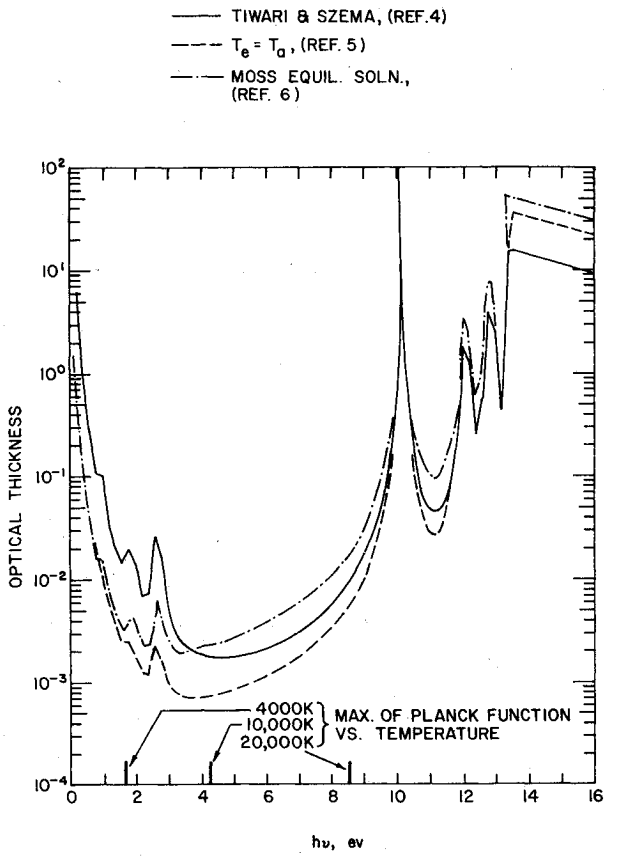

Fig. 3 Optical thickness of the stagnation shock layer as a function of radiation energy for ionization and thermal nonequilibrium, thermal equilibrium, and complete equilibrium.

function for representative shock-layer temperatures. The maximum occurs in the spectral region where the hydrogen shock layer is optically thin.

Radiative Flux at the Heat Shield

The radiative flux reaching the probe involves an integral over the source function such that

$$q_R(0,\nu) = -2\pi \int_{-1}^{0} \int_{0}^{\tau_\nu^o} S_\nu(t_\nu) \exp(t_\nu/\mu)\, dt_\nu\, d\mu. \qquad (1)$$

Using the tangent-slab approximation and assuming the shock layer to be optically thin, one obtains[7]

$$q_R(0,\nu) = -2\pi \int_{0}^{\delta_0} \frac{2h\nu^3}{c^2} n_H(2)\, \sigma_{2f} \exp(-h\nu/kT_e)\, dy. \qquad (2)$$

Thus, the radiative flux is strongly dependent on T_e and $n_H(2)$. The value of σ_{2f} is $15.8\times10^{-18}\ (h\nu_2/h\nu)^2$ cm^3, where $h\nu_2$ is 3.4 eV for hydrogen and $h\nu$ is the photon energy in eV units.[8]

Tiwari and Szema[3,4] assumed Boltzmann population distributions for the electronic states (excitation equilibrium) at the local value of T_e; consequently, the source function was the Planck function. Thus, they considered thermal and ionization nonequilibrium. They evaluated the excited state populations, source function, and absorption coefficient at T_e and used the 58-step spectral radiation model developed by Zoby et al.,[9] who also assumed that the atomic electronic states were Boltzmann populated.

For the solutions of Tiwari and Szema, T_e is high behind the shock. This increases the exponential term and $n_H(2)$ in Eq. (2) Thus, the finite-rate ionization solutions produce a large radiative flux.

In the equilibrium case, the temperature and the number of hydrogen atoms are lower than they are for the finite-ionization-rate case just behind the shock. See Fig. 2. Consequently, the contribution of the gas near the shock to the radiative flux is reduced. Near the body, T_e and $n_H(2)$ are about the same for the equilibrium and finite-ionization-rate solutions; therefore, the radiative flux from this part of the shock layer is about the same. Thus, Tiwari and Szema predicted that finite-rate ionization and thermal nonequilibrium increased the radiative flux compared to its equilibrium value.

Table 1 Population of the first excited state of atomic hydrogen for a Boltzmann distribution at T_e, or for equilibrium with electrons at T_e

η	T_e, K	n_H, 1/cm^3	n_e, n_H^+ 1/cm^3	$n_H(2)$,[a] 1/cm^3	$n_H(2)$,[b] 1/cm^3
1.000	20,000	8.39×10^{17}	4.66×10^{15}	7.93×10^{15}	9.14×10^{10}
0.950	19,500	8.49×10^{17}	9.99×10^{15}	7.67×10^{15}	4.59×10^{11}
0.900	19,100	8.22×10^{17}	3.64×10^{16}	6.57×10^{15}	6.57×10^{12}
0.875	18,700	8.26×10^{17}	6.60×10^{16}	5.79×10^{15}	2.33×10^{13}
0.850	18,400	8.16×10^{17}	8.62×10^{16}	5.17×10^{15}	4.21×10^{13}
0.825	18,000	8.19×10^{17}	1.34×10^{17}	4.51×10^{15}	1.11×10^{14}
0.800	17,000	8.20×10^{17}	1.53×10^{17}	3.08×10^{15}	1.77×10^{14}

[a] $n_H(2)$ For Boltzmann population distribution at T_e (Tiwari and Szeman assumption).
[b] $n_H(2)$ In equilibrium with n_e at T_e (Leibowitz and Kuo assumption).

The nonequilibrium solutions of Leibowitz and Kuo yield small values of $n_H(2)$ behind the shock compared to the Boltzmann distribution (equilibrium) value, because they considered not only thermal nonequilibrium and finite ionization, but also finite excitation. According to Eq. (2) low values of $n_H(2)$ decrease the radiative flux relative to equilibrium. Thus, Leibowitz and Kuo predicted that nonequilibrium reduces the radiative flux.

Table 1 gives values of $n_H(2)$ for the assumption that it is Boltzmann populated at T_e or that it is populated in equilibrium with n_e. The necessary data for T_e, n_H, and n_e were obtained from the solution of Tiwari and Szema shown in Figs. 1 and 2. Note that for the Boltzmann distribution, $n_H(2)$ is much greater than it is for the assumption that $n_H(2)$ and n_e exist in equilibrium at T_e. The assumptions used to calculate $n_H(2)$ are the major reasons for the opposite conclusions of Tiwari and Szema and Leibowitz and Kuo.

The discussion to this point has been limited to the optically thin approximation and the Balmer region of the spectrum; however, the conclusions are generally valid. Figure 3 shows that the ground state continuum radiation is optically thick; thus, only the gas near the body contributes to radiative heating of the body in that spectral region. The atomic line transitions are also optically thick near the line center, so the line centers contribute to radiative heating only if the radiation is emitted close to the body. The free-free continuum transitions occur mainly in the spectral range below 2 eV. The free-free continuum radiation can be important; however, at the temperatures of interest its contribution to the flux is small, because of its small source function. Consequently, the radiative heating comes mainly from the Balmer region of the spectrum, where the shock layer is optically thin, and the above approximations hold.

Acknowledgment

This research was supported by NASA Langley Research Center, Hampton, Va., under Contract NASA NAG 1-125.

References

[1]Leibowitz, L.P., "Measurements of the Structure of an Ionizing Shock Wave in a Hydrogen-Helium Mixture," *Physics of Fluids,* Vol. 16, 1973, p. 59.

[2]Leibowitz, L.P. and Kuo, Ta-Jin, "Ionizational Nonequilibrium Heating During Outer Planetary Entries," *AIAA Journal,* Vol. 14, Sept. 1976, p. 1324.

[3]Tiwari, S.N. and Szema, K.Y., "Effects of Precursor Heating on Chemical and Radiative Nonequilibrium Viscous Flow Around a Jovian Entry Body," *Progress in Astronautics and Aeronautics: Outer Planet Entry Heating and Thermal Protection,* Vol. 64, edited by R. Viskanta, AIAA, New York, 1979, pp. 129-146.

[4]Tiwari, S.N. and Szema, K.Y., "Effects of Precursor Heating on Radiating and Chemically Reacting Viscous Flow Around a Jovian Entry Body," NASA CR-3186, Sept. 1979.

[5]Zoby, E.V. and Moss, J.M., "Preliminary Thermal Analysis for Saturn Entry," *Progress in Astronautics and Aeronautics: Aerothermodynamics and Planetary Entry,* Vol. 77, edited by A.L. Crosbie, AIAA, New York, 1981, pp. 374-395.

[6]Moss, J.M., "A Study of the Aerothermal Entry Environment for the Galileo Probe," *Progress in Astronautics and Aeronautics: Entry Heating and Thermal Protection,* Vol. 69, edited by W.B. Olstad, AIAA, New York, 1980, pp. 3-25.

[7]Nelson, H.F., "Effect of a Finite Ionization Rate on the Radiative Heating of Outer Planet Atmospheric Entry Probes," NASA CR-3577, June 1982.

[8]Zel'dovich, Ya. B. and Raizer, Yu. P., *Physics of Shock Waves and High-Temperature Hydrodynamic Phenomena,* Academic Press, New York, 1966.

[9]Zoby, E.V., Sutton, K., Olstad, W.B. and Moss, J.M., "An Approximate Inviscid Radiating Flow-Field Analysis for Outer Planet Entry Probes," *Progress in Astronautics and Aeronautics: Outer Planet Entry Heating and Thermal Protection,* Vol. 64, edited by R. Viskanta, AIAA, New York, 1979, pp. 42-64.

Effect of Low Reynolds Number Turbulence Amplification on the Galileo Probe Flowfield

R. N. Gupta* and J. N. Moss†
NASA Langley Research Center, Hampton, Virginia

Introduction

IN a recent paper, Moss and Simmonds[1] presented the forebody flowfield solutions for Jupiter entry conditions for a 335-kg probe. These results for the massive ablation conditions were obtained by using the two-layer algebraic eddy-viscosity model due to Cebeci.[2,3] In this model of turbulence, the inner law is based upon Prandtl's mixing-length concept and the outer law employs the Clauser-Klebanoff expression. A value of 0.4 for the von Kármán constant k_1 appearing in the inner law and a value of 0.0168 for the constant k_2 appearing in the outer Clauser-Klebanoff expression have been employed by Moss and Simmonds[1] as suggested by the earlier work of Ref. 3. It was obtained in Ref. 4 that the variations in the inner law expression (including in the value of k_1) do not affect the value of eddy viscosity for a massively blown shock layer substantially. For such flows, the outer eddy-viscosity expression seems to play a predominant role. In the study of Ref. 4, the Cebeci model of Ref. 3 with a constant value of $k_2 = 0.0168$ was employed as the baseline model. Recent experimental studies[5] for the unblown blunt-body viscous-shock-layer flows, however, suggest that a much higher value than 0.0168 might be needed to obtain an agreement between the predictions and experimentally measured eddy-viscosity values, as shown in Fig. 1. This appears to be the result of low Reynolds number effect, which contributes to the amplification of turbulence. According to Ref. 6, a value of s/δ‡ of about 30 to 50 is required to "wash out" the low Reynolds number effect. For the Galileo probe, where the flow is assumed to undergo transition instantaneously immediately downstream of the stagnation point owing to massive ablation, a typical value of s/δ is about 15 at the end of the forebody flowfield. Therefore the low Reynolds number effect is likely to persist for the entire length of the probe and may contribute to the amplification of turbulence more for a blown surface than for an unblown surface. The purpose of this study is to evaluate the impact of this effect on the Galileo probe surface-heating and mass-loss rates, which are critical to the probe's success.

Analysis

The extent of the low Reynolds number amplification is indicated in the figure inset in Fig. 2 (taken from Ref. 7) where the mixing length, $(l/\delta)_{max}$, was derived from the experimental velocity profiles for flat plates, cones, and cylinders. Also shown in the inset figure is an extrapolation to the curve of Ref. 7 for a value of δ^+ near 100. Here δ^+ is a measure of the Reynolds number based on boundary-layer thickness δ, friction velocity $U_\tau (= \sqrt{\tau_w/\rho_w})$, and wall conditions. Although the mixing-length amplification contained in Fig. 2 (obtained for the "wall" turbulent shear flows) is not strictly applicable for "free" turbulent shear

Received Nov. 3, 1982; revision received Jan. 7, 1983.

*NRC-Senior Research Associate, Aerothermodynamics Branch, Space Systems Division. Member AIAA.

†Research Leader, Aerothermodynamics Branch, Space Systems Division. Member AIAA.

‡Various symbols used in this paper have meanings similar to those of Refs. 1 and 3.